



Title	Single-Crystal Cobalt Phosphide Nanorods as a High-Performance Catalyst for Reductive Amination of Carbonyl Compounds
Author(s)	Sheng, Min; Fujita, Shu; Yamaguchi, Sho et al.
Citation	JACS Au. 2021, 1(4), p. 501-507
Version Type	VoR
URL	<a href="https://hdl.handle.net/11094/79297">https://hdl.handle.net/11094/79297</a>
rights	© 2021 The Authors. Published by American Chemical Society. This article is licensed under a Creative Commons Attribution-NonCommercial-NoDerivatives 4.0 International License.
Note	

*The University of Osaka Institutional Knowledge Archive : OUKA*

<https://ir.library.osaka-u.ac.jp/>

The University of Osaka

# Single-Crystal Cobalt Phosphide Nanorods as a High-Performance Catalyst for Reductive Amination of Carbonyl Compounds

Min Sheng, Shu Fujita, Sho Yamaguchi, Jun Yamasaki, Kiyotaka Nakajima, Seiji Yamazoe, Tomoo Mizugaki, and Takato Mitsudome\*



Cite This: <https://doi.org/10.1021/jacsau.1c00125>



Read Online

ACCESS |



Metrics & More



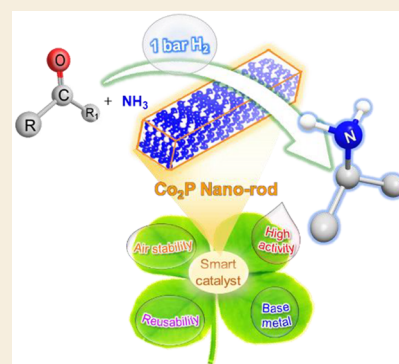
Article Recommendations



Supporting Information

**ABSTRACT:** The development of metal phosphide catalysts for organic synthesis is still in its early stages. Herein, we report the successful synthesis of single-crystal cobalt phosphide nanorods (Co<sub>2</sub>P NRs) containing coordinatively unsaturated Co–Co active sites, which serve as a new class of air-stable, highly active, and reusable heterogeneous catalysts for the reductive amination of carbonyl compounds. The Co<sub>2</sub>P NR catalyst showed high activity for the transformation of a broad range of carbonyl compounds to their corresponding primary amines using an aqueous ammonia solution or ammonium acetate as a green amination reagent at 1 bar of H<sub>2</sub> pressure; these conditions are far milder than previously reported. The air stability and high activity of the Co<sub>2</sub>P NRs is noteworthy, as conventional Co catalysts are air-sensitive (pyrophorous) and show no activity for this transformation under mild conditions. P-alloying is therefore of considerable importance for nanoengineering air-stable and highly active non-noble-metal catalysts for organic synthesis.

**KEYWORDS:** cobalt, phosphide, reductive amination, aldehyde, ketone



## INTRODUCTION

Heterogeneous metal catalysts are a part of key technologies in automobile exhaust gas cleaning, energy conversion, and storage, including fuel cells, water-splitting, N<sub>2</sub> reduction, and other industrially important reactions, such as petrochemical manufacturing and fine chemical synthesis.<sup>1–4</sup> The precise fabrication of metal nanomaterials through control over their morphologies (size and shape), doping with heteroatoms, and alloying with additional metals or non-metal elements considerably improves their catalytic performances.<sup>5–8</sup> In this context, less common metal–metalloid alloys, specifically metal phosphide nanoalloys, have attracted attention as a new class of hydrotreating catalysts and electro- and photocatalysts for energy conversion.<sup>6,9–14</sup> It is also predicted that the introduction of P atoms into metals can significantly improve the catalytic properties of conventional metal catalyst systems for energy and environmental applications.<sup>15</sup> However, the use of metal phosphide catalysts in organic synthesis is still in the early stages of development, as examples of these are limited.<sup>16–20</sup> Nevertheless, we recently reported the catalytic activity of nickel and cobalt phosphide nanoalloys for the transformation of biofuranic aldehydes to diketones and the hydrogenation of nitriles to primary amines, respectively, exhibiting turnover numbers (TONs) an order of magnitude higher than those of conventional non-noble-metal catalysts.<sup>21,22</sup> Based on the above studies, we concluded that “phosphorus-alloying (P-alloying)” has two important roles in non-noble-metal-catalyzed organic transformations. One is its

ability to stabilize low valent metals. X-ray absorption fine structure (XAFS) studies have shown that metal phosphide nanoalloys retain their metallic states in air.<sup>21–23</sup> The other is the ligand effect. Density functional theory (DFT) calculations revealed that P-alloying can modulate the electronic state of the metal species and increase its *d*-electron density near the Fermi level. This effect imparts the metal with a high ability to hydrogenate.<sup>22</sup> Furthermore, we envisaged that P-alloying could be advantageous for the creation of well-defined catalytically active species in the crystalline metal phosphide that favor selective reactions. This is in contrast to conventional heterogeneous catalysts, which have multiple ill-defined active sites that result in inferior catalytic performance. These results encouraged us to further investigate the catalytic potential of metal phosphides in other valuable molecular transformations.

Primary amines are essential feedstocks and key intermediates in the manufacture of pharmaceuticals, dyes, polymers, and detergents.<sup>24–26</sup> Reductive amination of carbonyl compounds with ammonia and hydrogen represents one of the most sustainable methods to synthesize primary amines

Received: March 16, 2021

with high atom efficiency, as the carbonyls and reagents are easily available and inexpensive, and theoretically, only water is formed as a byproduct. To date, various metal catalysts have been developed for reductive amination.<sup>27–40</sup> Among them, low-cost and earth-abundant metal-based catalysts such as nickel and/or cobalt sponge metal catalysts, e.g., Raney catalysts, are widely employed in industrial reductive amination reactions.<sup>41–43</sup> However, these catalysts are highly air-sensitive (pyrophorous) and easily deactivated during storage, requiring anaerobic handling to avoid oxidative degradation during the activation, operation, separation, and reuse steps of the catalysts. Moreover, these catalysts require harsh reaction conditions, e.g., high H<sub>2</sub> pressures, and their applicability for converting carbonyl compounds is limited. Therefore, the development of air-stable earth-abundant metal catalyst alternatives to sponge metal catalysts for the reductive amination of carbonyl compounds is highly challenging and in great demand. In this regard, significant progress was made by Beller et al., who recently reported that coating non-noble-metal nanoparticles (NPs) with N-doped carbon materials is an attractive strategy to produce air-stable non-noble-metal catalysts for various hydrogenation reactions.<sup>44–48</sup> Based on this concept, air-stable and reusable Ni-, Co-, and Fe-based catalysts for reductive amination reactions were developed (Figure 1a).<sup>34–38</sup> To date, there is no catalyst design strategy

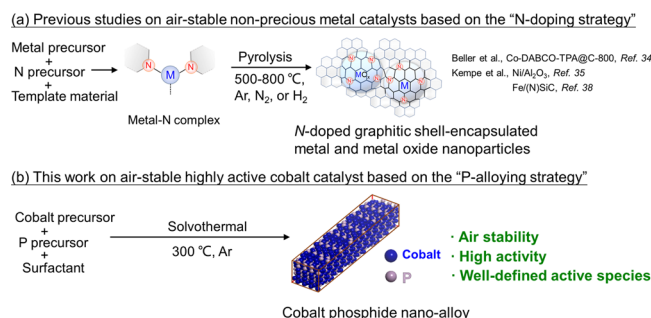


**Figure 1.** Air-stable non-precious metal catalysts for reductive amination based on (a) an N-doping strategy and (b) a P-alloying strategy.

available to develop air-stable base metal catalysts for reductive aminations, except for the aforementioned "N-doping strategy," and flammable ammonia gas and/or high H<sub>2</sub> pressures are still required to promote the amination reaction. Moreover, the active surface sites of these non-noble-metal catalysts are shielded due to encapsulation by N-doped carbon layers; thus, the stability of the NPs is achieved at the expense of their activity. Therefore, there is still considerable interest in establishing innovative, efficient, and sustainable catalyst technology to overcome the trade-off between stability and activity of non-noble-metal NPs for reductive amination. Herein, we report the novel synthesis of single-crystal cobalt phosphide nanorods (Co<sub>2</sub>P NRs) based on the "P-alloying strategy." Co<sub>2</sub>P NRs serve as smart catalysts, which exhibit both high activity and air stability in the reductive amination of carbonyl compounds with ammonia reagents (Figure 1b). A wide range of carbonyl compounds were converted to their corresponding primary amines with high efficiency and at a notably low H<sub>2</sub> pressure. This is the first example of a metal phosphide for promoting reductive amination.

## RESULTS AND DISCUSSION

The Co<sub>2</sub>P NRs were synthesized according to a previously reported method with slight modifications (e.g., the metal precursor used).<sup>22</sup> Cobalt(II) acetylacetonate [Co(acac)<sub>3</sub>] was added to 1-octadecene in the presence of hexadecylamine and triphenylphosphite. The mixture was stirred under an argon atmosphere, while the temperature was increased to 300 °C, which generated a black colloidal solution. The product was collected by centrifugation and washed to afford the Co<sub>2</sub>P NRs. The representative transmission electron microscopy (TEM) images show that the prepared Co<sub>2</sub>P NPs have a uniform nanorod morphology with a diameter of ~10 nm and length in the range of 50–150 nm (Figures 2a,b). Figure 2c

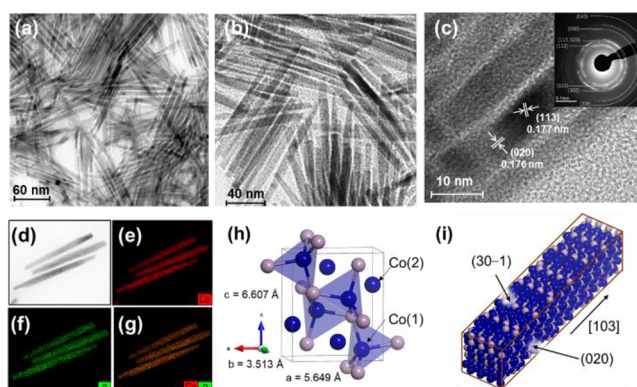


**Figure 2.** (a,b) TEM images of the Co<sub>2</sub>P NRs showing a rod-like morphology. (c) HR-TEM image of the Co<sub>2</sub>P NRs with the inset illustrating the corresponding SAED pattern. (d) STEM image of the Co<sub>2</sub>P NRs. Elemental mapping images of (e) Co and (f) P. (g) Composite overlay image of (e) and (f). (h) Unit cell of Co<sub>2</sub>P (ICSD 94379). (i) Proposed crystal structure of the Co<sub>2</sub>P NR.

displays a high-resolution TEM (HR-TEM) image that includes distinct fringes. The measured lattice fringe *d*-spacing values are 0.176 and 0.177 nm, which correspond to the (020) and (113) surfaces, respectively (Figure 2c). Hence, the growth direction is assigned to [103], which is different from the growth direction of the Co<sub>2</sub>P structure previously reported.<sup>49</sup> Figure 2c (inset) shows the selected area electron diffraction (SAED) patterns of the NRs (Figure S1). The diffraction pattern can be indexed based on the Co<sub>2</sub>P orthorhombic structure (space group: *Pnma*; lattice parameters: *a* = 5.649 Å, *b* = 3.513 Å, *c* = 6.607 Å), revealing the single-crystalline nature of the synthesized Co<sub>2</sub>P NRs (Figure 2h).<sup>50</sup> Elemental mapping using scanning transmission electron microscopy (STEM) confirms the homogeneous distribution of the Co and P elements (Figures 2e–g). In addition, the corresponding energy-dispersive X-ray (EDX) spectrum demonstrates that the stoichiometric Co-to-P ratio is close to 2:1 (Figure S2). These results clearly support the successful synthesis of single-crystal Co<sub>2</sub>P NRs containing large amounts of Co(2) content on the surfaces ((020), (30-1)), as illustrated in Figure 2i.

To gain more insight into the Co species present in the Co<sub>2</sub>P NRs, Co *K*-edge XAFS analysis was conducted in air atmosphere. The edge positions of the X-ray absorption near-edge structure (XANES) spectra of the Co<sub>2</sub>P NRs, bulk Co<sub>2</sub>P, and CoP NPs are presented in Figure 3. The spectra of the cobalt phosphides with varying P contents differ from that of CoO but are similar to that of Co foil, indicating that the Co

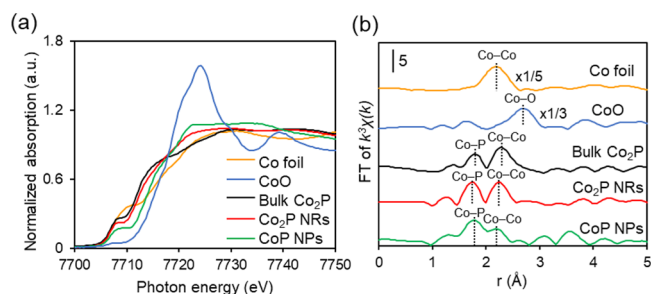


**Figure 3.** Co K-edge (a) XANES and (b) FT-EXAFS spectra of Co foil, CoO, bulk Co<sub>2</sub>P, Co<sub>2</sub>P NRs, and CoP NPs.

species in the cobalt phosphides is in the metallic state (Figure 3a). This air-stable metallic nature of the Co<sub>2</sub>P NRs is well supported by the X-ray photoelectron spectroscopy (XPS) analysis of the air-exposed Co<sub>2</sub>P NRs. The obtained Co 2p spectrum includes peaks at 777.8 and 792.8 eV, which are close to or slightly more negative than those of metallic Co 2p<sub>3/2</sub> (777.9 eV) and Co 2p<sub>1/2</sub> (793.5 eV) (Figure S3). Figure 3b shows the Fourier transform extended X-ray absorption fine structure (FT-EXAFS) spectra of the Co foil, CoO, bulk Co<sub>2</sub>P, Co<sub>2</sub>P NRs, and CoP NPs. The Co–P and Co–Co bonds appear at 1.6–2.0 and 2.0–2.5 Å, respectively, for bulk Co<sub>2</sub>P, the Co<sub>2</sub>P NRs, and CoP NPs. The absence of Co–O bonds indicates that the Co<sub>2</sub>P NRs are not oxidized in air, which is consistent with the XANES and XPS analysis results (Figures 3a and S3). Curve fitting analysis was conducted to determine the local structure of the Co<sub>2</sub>P NRs. The Co<sub>2</sub>P NRs and cobalt phosphide references have longer Co–Co bonds (2.56–2.60 Å) than Co foil (2.49 Å) (Table S1), because the Co–Co bonds are present in the tetrahedral CoP<sub>4</sub> network with vertex and edge sharing in orthorhombic Co<sub>2</sub>P (Figure 2h). The noticeable difference between the Co<sub>2</sub>P NRs and bulk Co<sub>2</sub>P is the coordination number (CN) ratio, CN<sub>Co–Co</sub>/CN<sub>Co–P</sub>. The CN<sub>Co–Co</sub>/CN<sub>Co–P</sub> ratio (1.6) of the Co<sub>2</sub>P NRs is smaller than that of bulk Co<sub>2</sub>P (2.0), with the ideal value (1.8) calculated from the crystal structure of orthorhombic Co<sub>2</sub>P. The small CN<sub>Co–Co</sub>/CN<sub>Co–P</sub> ratio of the Co<sub>2</sub>P NRs indicates that a high number of coordinatively unsaturated Co–Co sites is present on the nanorod surfaces, which is induced by the formation of the rod-shape morphology with a high content of Co(2), as shown in Figure 2i.

Initially, the catalytic activity of the Co<sub>2</sub>P NRs was investigated for the reductive amination of a model substrate, benzaldehyde (1a), in water using three types of amination sources (an aqueous ammonia solution (aq. NH<sub>3</sub>), gaseous ammonia (NH<sub>3</sub> gas), and ammonium acetate (NH<sub>4</sub>OAc)) at 10 bar H<sub>2</sub> and 100 °C for 10 h (Table 1). Notably, the Co<sub>2</sub>P NRs showed high catalytic activities when using aq. NH<sub>3</sub> and NH<sub>3</sub> gas, producing the corresponding benzylamine (2a) as the sole product in 93 and 88% yields, respectively (entries 1 and 2), while NH<sub>4</sub>OAc provided a low yield of 2a, accompanied by the formation of benzyl alcohol (4a) (entry 3). At a lower H<sub>2</sub> pressure of 5 bar, the Co<sub>2</sub>P NRs also generated high 2a yields when using aq. NH<sub>3</sub> (entry 4). The Co<sub>2</sub>P NRs were even active at just 1 bar of H<sub>2</sub> pressure, selectively affording 2a in a high yield (entry 5). This is the first example of a cobalt catalyst that can promote reductive amination under ambient H<sub>2</sub> pressure. A comparison experiment between the Co<sub>2</sub>P NRs and state-of-the-art Ni/Al<sub>2</sub>O<sub>3</sub><sup>35</sup> under the same ambient H<sub>2</sub> pressure conditions was also

**Table 1.** Reductive Amination of Benzaldehyde with Co<sub>2</sub>P NRs and Other Cobalt Catalysts<sup>a</sup>

entry	catalyst	H <sub>2</sub>	NH <sub>3</sub> source	time (h)	yield (%) <sup>b</sup>		
					2a	3a	4a
1	Co <sub>2</sub> P NRs	10	aq. NH <sub>3</sub>	10	93	0	0
2 <sup>c</sup>	Co <sub>2</sub> P NRs	10	NH <sub>3</sub> gas	10	88	0	0
3 <sup>d</sup>	Co <sub>2</sub> P NRs	10	NH <sub>4</sub> OAc	10	15	0	73
4	Co <sub>2</sub> P NRs	5	aq. NH <sub>3</sub>	10	94	0	0
5	Co <sub>2</sub> P NRs	1	aq. NH <sub>3</sub>	12	90	0	1
6 <sup>e</sup>	Co <sub>2</sub> P NRs	40	aq. NH <sub>3</sub>	48	87	0	0
7	bulk Co <sub>2</sub> P	1	aq. NH <sub>3</sub>	12	0	0	0
8	CoP NPs	1	aq. NH <sub>3</sub>	12	0	12	0
9	sponge Co	1	aq. NH <sub>3</sub>	12	0	11	3
10	Co/SiO <sub>2</sub>	1	aq. NH <sub>3</sub>	12	0	0	0
11	Co/SiO <sub>2</sub> -Red	1	aq. NH <sub>3</sub>	12	0	0	0

<sup>a</sup>Reaction conditions: Co catalyst (Co: 0.05 mmol), benzaldehyde (0.5 mmol), aq. NH<sub>3</sub> 25% (3 mL), 100 °C. <sup>b</sup>Determined by gas chromatography–mass spectrometry (GC–MS) using an internal standard. <sup>c</sup>NH<sub>3</sub> gas (2.5 bar), water (3 mL). <sup>d</sup>NH<sub>4</sub>OAc (0.2 g), water (3 mL). <sup>e</sup>Co<sub>2</sub>P NRs (Co: 0.02 mmol), benzaldehyde (1.0 mmol), aq. NH<sub>3</sub> 25% (3 mL), room temperature (25 °C), 48 h.

carried out, and the Co<sub>2</sub>P NRs showed a higher yield (79 vs 6%) of 2a, revealing the superior activity of the Co<sub>2</sub>P NRs (Scheme S1). We further investigated the catalytic potential of the Co<sub>2</sub>P NRs at room temperature using a 2 mol % catalyst loading. The Co<sub>2</sub>P NRs could catalyze the reductive amination of 1a at room temperature, producing 2a in 87% yield (entry 6); this is the first example of non-noble-metal-catalyzed reductive amination under ambient temperature conditions. These results clearly demonstrate the distinct performance of the Co<sub>2</sub>P NRs from reported non-noble-metal catalysts requiring high H<sub>2</sub> pressures or high temperatures (Table S2 and Scheme S1).

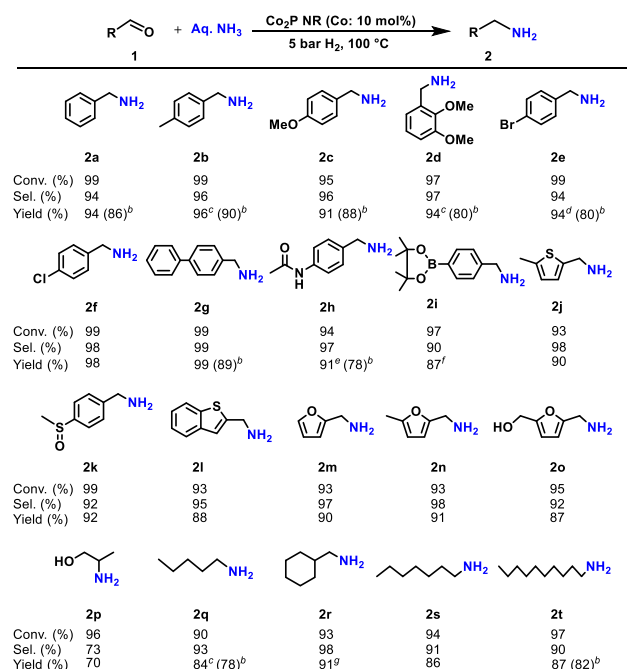
With the Co<sub>2</sub>P NRs in hand, the reductive amination of functionalized aldehydes was investigated using aq. NH<sub>3</sub> in H<sub>2</sub> atmosphere; the results are shown in Scheme 1. The Co<sub>2</sub>P NRs exhibited high activity toward various aromatic and aliphatic aldehydes, producing the corresponding primary amines in high yields. Furthermore, various functional groups, such as halogen, methoxy, amide, and boronic ester moieties, were tolerant under these reaction conditions, providing the corresponding primary amines in excellent yields. Although it is well-known that sulfur compounds often strongly coordinate to the active sites of metals, resulting in significant deactivation of the catalysts, the Co<sub>2</sub>P NR catalyst could be used for sulfur-containing carbonyl substrates such as 1j, 1k, and 1l.

Moreover, biomass-derived substrates, such as 1m, 1n, 1o, and 1p, were transformed to their corresponding primary amines in high yields.

The applicability of the Co<sub>2</sub>P NRs was further explored in the reductive aminations of ketones, which is more challenging than that of aldehydes owing to the hydrogenation of more sterically hindered imine intermediates. Screening of the amination reagents in acetophenone amination revealed that NH<sub>4</sub>OAc in ethanol provided the best corresponding amine yield (83%) and selectivity (100%), while using aq. NH<sub>3</sub> and NH<sub>3</sub> gas resulted in moderate amine yields (Table S3). Further screening experiments revealed that a Co<sub>2</sub>P NR/ketone/NH<sub>4</sub>OAc ratio of 1:10:60 in ethanol provided the optimal



**Scheme 1. Substrate Scope for the Co<sub>2</sub>P NR-Catalyzed Reductive Amination of Aldehydes with Aqueous NH<sub>3</sub><sup>a</sup>**



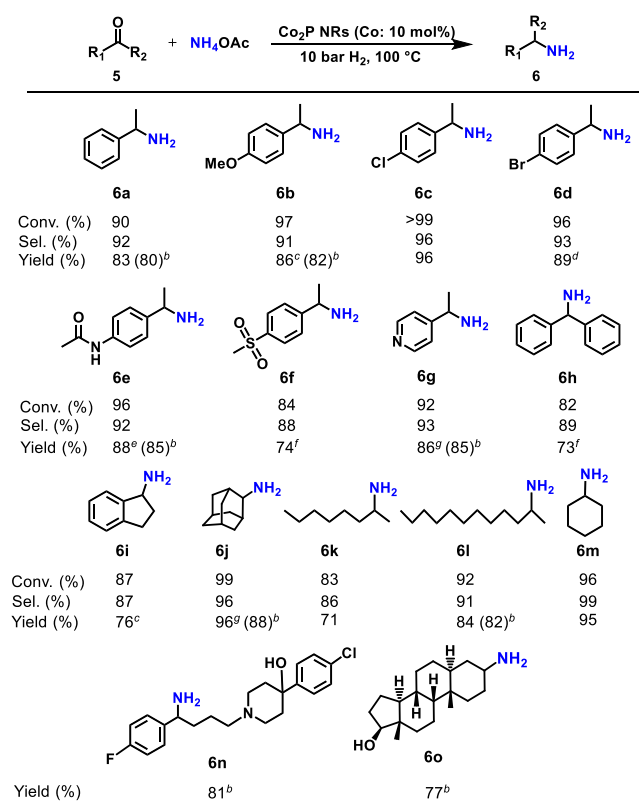
<sup>a</sup>Reaction conditions: Co<sub>2</sub>P NRs (4.0 mg), aldehyde (0.5 mmol), aq. NH<sub>3</sub> 25% (3 mL), 5 bar H<sub>2</sub>, 100 °C, 10 h. Yields were determined by GC–MS using an internal standard. <sup>b</sup>Isolated yield as a hydrochloride salt. <sup>c</sup>120 °C, 6 h. <sup>d</sup>70 °C. <sup>e</sup>80 °C, 10 bar H<sub>2</sub>. <sup>f</sup>80 °C. <sup>g</sup>Aq. NH<sub>3</sub> 25% (5 mL), 120 °C.

reaction conditions (Table S3). The Co<sub>2</sub>P NRs were highly active for a wide range of ketones under the optimized conditions (Scheme 2). Aromatic and heteroaromatic ketones bearing diverse functional groups, such as methoxy, halogen, amide, methyl, and sulfone functionalities, were efficiently aminated. Aliphatic and alicyclic ketones were also converted to their corresponding primary branched amines in high yields. Moreover, the Co<sub>2</sub>P NRs could aminate structurally complex ketones including steroid-based molecules, such as **5n** and **5o**, demonstrating the prominent catalytic activity of the Co<sub>2</sub>P NRs.

To investigate additional advantages of the use of the Co<sub>2</sub>P NRs, some typical experiments were performed. Scheme 3 shows the substrate generality of the present amination method using the Co<sub>2</sub>P NRs at 1 bar H<sub>2</sub> pressure. Several aldehydes and ketones were converted to their corresponding primary amines in high yields, demonstrating that the use of the Co<sub>2</sub>P NRs provides a convenient and general amination method for carbonyl compounds under mild reaction conditions.

The Co<sub>2</sub>P NRs operated well under scale-up conditions: 2.4 g of **1a** was aminated to produce the corresponding hydrochloride salt in 83% yield with a high turnover number (TON) that exceeds 1000 at 40 bar H<sub>2</sub> and 130 °C (Scheme 4). This TON value is the highest among homogeneous and heterogeneous non-noble-metal-based catalysts developed to date, demonstrating the distinct activity and stability of the Co<sub>2</sub>P NRs, even with prolonged heating and elevated temperatures (Table S2). Another advantage of the Co<sub>2</sub>P NRs is their convenient recyclability and high reusability. Conventional non-noble-metal-based catalysts are generally

**Scheme 2. Substrate Scope for the Co<sub>2</sub>P NR-Catalyzed Reductive Amination of Ketones with Ammonium Acetate<sup>a</sup>**



<sup>a</sup>Reaction conditions: Co<sub>2</sub>P NRs (4.0 mg), ketone (0.5 mmol), NH<sub>4</sub>OAc (0.2 g), ethanol (3 mL), 10 bar H<sub>2</sub>, 100 °C, 12 h. Yields were determined by GC–MS using an internal standard. <sup>b</sup>Isolated yield as a hydrochloride salt. <sup>c</sup>NH<sub>4</sub>OAc (0.1 g), 20 bar H<sub>2</sub>, 110 °C. <sup>d</sup>110 °C. <sup>e</sup>NH<sub>4</sub>OAc (0.1 g), 80 °C. <sup>f</sup>20 bar H<sub>2</sub>, 110 °C. <sup>g</sup>NH<sub>4</sub>OAc (0.1 g).

sensitive to air and require strict anaerobic conditions during the recycling process. In contrast, after the reaction, the Co<sub>2</sub>P NRs were easily recovered by simple filtration under air and reused without loss of activity, even after the fourth cycle, showing high durability (Figure 4). We further investigated the initial reaction rate during the recycling experiments. Similar reaction rates (gray diamonds in Figure 4) were achieved when using the reused catalyst and the fresh catalyst. Furthermore, TEM images of the used Co<sub>2</sub>P NRs reveal that the Co<sub>2</sub>P NRs does not aggregate and the size and shape of the Co<sub>2</sub>P NRs are unchanged (Figure S4). No significant changes are observed in the Co<sub>2</sub>P NR catalyst after reuse, as confirmed by EDX, X-ray diffraction, XANES, EXAFS, and curve fitting (Figures S2, S5, S6, S7, and S8, respectively). These analyses strongly prove the high stability of the Co<sub>2</sub>P NRs.

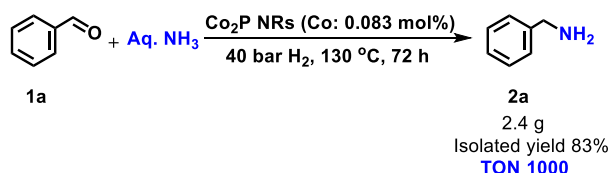
Finally, the reaction pathway of the Co<sub>2</sub>P NR-catalyzed reductive amination was investigated by monitoring the products. The time-course data of the benzaldehyde amination (**1a**) with aq. NH<sub>3</sub> and H<sub>2</sub> using the Co<sub>2</sub>P NRs show that the amount of **1a** significantly decreases at the initial stage with the production of the *N*-benzylidenebenzylamine intermediate (**3a**) through the condensation of **1a** and benzylamine (**2a**) (Figure 5). The maximum yield of **3a** is obtained after 2 h, which then gradually decreases with an increase in the yield of **2a**, indicating that the transformation of **3a** to **2a** is the rate-determining step. Based on these results, a possible reaction

### Scheme 3. Reductive Amination of Carbonyl Compounds by the Co<sub>2</sub>P NRs at 1 bar H<sub>2</sub><sup>a</sup>

$R_1$		$R_2$		$R_1$		$R_2$	
<b>2a</b>		<b>2c</b>		<b>2e</b>		<b>2f</b>	
Conv. (%) 98		99		98		88	
Sel. (%) 96		93		95		84	
Yield (%) 94		93		93		74	
<b>2g</b>		<b>2h</b>		<b>2q</b>			
Conv. (%) 99		97		>99			
Sel. (%) 95		95		89			
Yield (%) 95		92		89			
<b>6a</b>		<b>6b</b>		<b>6m</b>		<b>6n</b>	
Conv. (%) 82		95		89		78	
Sel. (%) 89		95		92		92	
Yield (%) 73 <sup>b</sup>		90 <sup>b</sup>		82 <sup>b</sup>		72 <sup>c</sup>	

<sup>a</sup>Reaction conditions: Co<sub>2</sub>P NRs (4.0 mg), substrate (0.5 mmol), 1 bar H<sub>2</sub>, aq. NH<sub>3</sub> 25% (3 mL), 100 °C, 12 h. Yields were determined by GC–MS using an internal standard. <sup>b</sup>NH<sub>4</sub>OAc (0.1 g), ethanol (3 mL). <sup>c</sup>NH<sub>4</sub>OAc (0.15 g), ethanol (3 mL), 110 °C, 20 h.

### Scheme 4. Gram-Scale Experiment of the Reductive Amination of 1a Using the Co<sub>2</sub>P NRs<sup>a</sup>



<sup>a</sup>Reaction conditions: Co<sub>2</sub>P NRs (1.1 mg, Co: 0.018 mmol), **1a** (2.4 g), aq. NH<sub>3</sub> 25% (40 mL), ethanol (20 mL), 40 bar H<sub>2</sub>, 130 °C, 72 h.

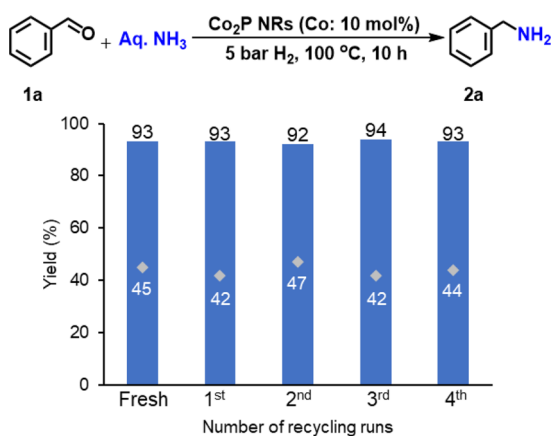


**Figure 4.** Reusability of the Co<sub>2</sub>P NR-catalyzed reductive amination of **1a** with aq. NH<sub>3</sub>. Reaction conditions: Co<sub>2</sub>P NRs (4.0 mg), **1a** (0.5 mmol), aq. NH<sub>3</sub> 25% (3 mL), 5 bar H<sub>2</sub>, 100 °C, 10 h. The initial reaction rate experiments (gray diamonds) were conducted under the same reaction conditions for 5 h. Yields were determined by GC–MS using an internal standard.

pathway for the transformation of **1a** to **2a** using the Co<sub>2</sub>P NRs is proposed, as shown in Scheme 5. First, the condensation of

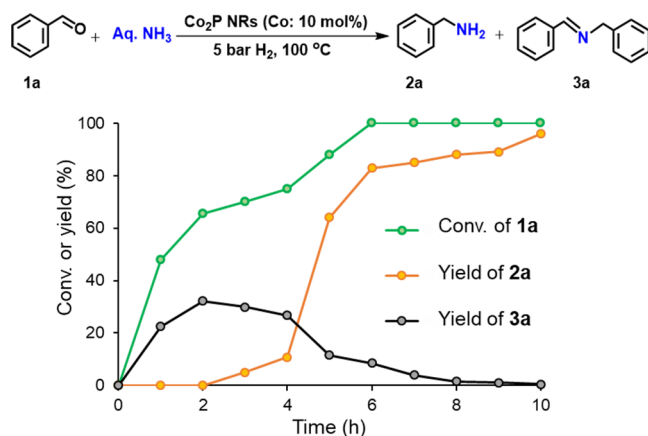
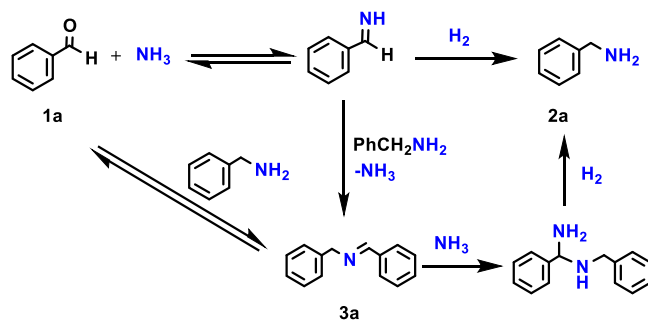


**Figure 5.** Time-course data of the Co<sub>2</sub>P NR-catalyzed reductive amination of **1a** with aq. NH<sub>3</sub>. Reaction conditions: Co<sub>2</sub>P NRs (4.0 mg), **1a** (0.5 mmol), aq. NH<sub>3</sub> 25% (3 mL), 5 bar H<sub>2</sub>, 100 °C, 10 h. Yields were determined by GC–MS using an internal standard.

### Scheme 5. Possible Reaction Pathway for the Co<sub>2</sub>P NR-Catalyzed Transformation of Benzaldehyde (**1a**) to Benzylamine (**2a**)



**1a** and NH<sub>3</sub> produces phenylmethanimine, which is then hydrogenated to **2a**. Then, the condensation of **1a** and **2a** rapidly generates **3a**. Subsequently, **3a** is gradually transformed into **2a**. It is reported that the addition of NH<sub>3</sub> to **3a** forms an unstable geminal amine, which is then hydrogenated to **2a**.<sup>51</sup> This is well-supported by the control experiments using **3a** as starting material, where the yield of **2a** increases in the presence of NH<sub>3</sub> (Figure S9). The high catalytic activity of the Co<sub>2</sub>P NRs is related to its high hydrogenation ability, i.e., the hydrogenation of phenylmethanimine to **2a** and **3a** to **2a**, which is derived from the rod-shaped morphology providing a high number of coordinatively unsaturated Co–Co surface sites. Furthermore, our recent study using DFT calculations revealed that P-alloying and nanosizing of Co significantly increases the *d*-electron density of Co near the Fermi level, which provides the high hydrogenation ability of the Co<sub>2</sub>P nanoparticles.<sup>22</sup> Hence, the Co<sub>2</sub>P NRs accelerate the hydrogenation of the intermediate imines and **3a**, resulting in high catalytic activity for the reductive amination of carbonyl compounds.

## CONCLUSION

We synthesized novel single-crystal Co<sub>2</sub>P NRs, which retain their air-stable metallic nature, containing coordinatively unsaturated Co–Co active sites. The well-ordered Co<sub>2</sub>P NRs serve as highly active and reusable heterogeneous catalysts for the reductive amination of various carbonyl compounds to the

corresponding primary amines using  $\text{NH}_3$  sources and  $\text{H}_2$ . The observed catalytic activity is superior to that of previously reported catalyst systems. Typically, the  $\text{Co}_2\text{P}$  NRs promote the amination under relatively mild conditions, even at 1 bar  $\text{H}_2$  pressure. This is the first example of both a metal phosphide promoting reductive amination and a cobalt catalyst operating at ambient  $\text{H}_2$  pressure. Furthermore, this solid catalyst is recoverable and reusable while maintaining its high catalytic activity and selectivity. Our findings demonstrate that the “P-alloying strategy” is a promising nanotechnology to develop a new class of stable and highly active non-noble-metal catalysts that can substitute conventional sponge metal catalysts. We believe that these less common metal phosphides also exhibit unique and high-performance activity in a broader field of reactions. “P-alloying” therefore provides a new avenue for greener and more sustainable synthesis of valuable chemicals.

## ■ ASSOCIATED CONTENT

### Supporting Information

The Supporting Information is available free of charge at <https://pubs.acs.org/doi/10.1021/jacsau.1c00125>.

Experimental details and catalyst characterization results (PDF)

## ■ AUTHOR INFORMATION

### Corresponding Author

**Takato Mitsudome** – Department of Materials Engineering Science, Graduate School of Engineering Science, Osaka University, Toyonaka, Osaka 560-8531, Japan; [orcid.org/0000-0002-0924-5616](https://orcid.org/0000-0002-0924-5616); Email: [mitsudom@cheng.es.osaka-u.ac.jp](mailto:mitsudom@cheng.es.osaka-u.ac.jp)

### Authors

**Min Sheng** – Department of Materials Engineering Science, Graduate School of Engineering Science, Osaka University, Toyonaka, Osaka 560-8531, Japan

**Shu Fujita** – Department of Materials Engineering Science, Graduate School of Engineering Science, Osaka University, Toyonaka, Osaka 560-8531, Japan

**Sho Yamaguchi** – Department of Materials Engineering Science, Graduate School of Engineering Science, Osaka University, Toyonaka, Osaka 560-8531, Japan; [orcid.org/0000-0002-0014-3218](https://orcid.org/0000-0002-0014-3218)

**Jun Yamasaki** – Research Center for Ultra-High Voltage Electron Microscopy, Osaka University, Ibaraki, Osaka 567-0047, Japan

**Kiyotaka Nakajima** – Institute for Catalysis, Hokkaido University, Sapporo 001-0021, Japan; [orcid.org/0000-0002-3774-3209](https://orcid.org/0000-0002-3774-3209)

**Seiji Yamazoe** – Department of Chemistry, Tokyo Metropolitan University, Hachioji, Tokyo 192-0397, Japan; [orcid.org/0000-0002-8382-8078](https://orcid.org/0000-0002-8382-8078)

**Tomoo Mizugaki** – Department of Materials Engineering Science, Graduate School of Engineering Science, Osaka University, Toyonaka, Osaka 560-8531, Japan; Innovative Catalysis Science Division, Institute for Open and Transdisciplinary Research Initiatives (ICS-OTRI), Osaka University, Suita, Osaka 565-0871, Japan; [orcid.org/0000-0001-5701-7530](https://orcid.org/0000-0001-5701-7530)

Complete contact information is available at:

<https://pubs.acs.org/doi/10.1021/jacsau.1c00125>

## ■ Author Contributions

T. Mit. wrote the paper and coordinated all the experimental investigations. M.S. designed and performed the experiments. S.F. and J.Y. performed the TEM measurements and analysis. S. Yamaz. performed the XAFS analysis. S. Yamag., K.N., and T. Miz. discussed the experiments and results. All authors commented critically on the manuscript and approved the final manuscript.

## ■ Funding

This work was supported by JSPS KAKENHI Grant Nos. 26105003, 17H03457, 18H01790, 20H02523, and 20H05879. This study was partially supported by the Cooperative Research Program of Institute for Catalysis, Hokkaido University (19A1002 and 20B1027). A part of this work was supported by the “Nanotechnology Platform Program” at Hokkaido University (A-20-HK-0011) and Nanotechnology Open Facilities in Osaka University (A-20-OS-0025), Ministry of Education, Culture, Sports, Science and Technology (MEXT), Japan.

## ■ Notes

The authors declare no competing financial interest.

## ■ ACKNOWLEDGMENTS

We would like to thank Dr. Ina (SPRING-8) for the XAFS measurements (2019A1390, 2019A1649, and 2019B1560) and R. Ota of Hokkaido University for the STEM analysis.

## ■ REFERENCES

- (1) Kondratenko, E. V.; Mul, G.; Baltrusaitis, J.; Larrazábal, G. O.; Pérez-Ramírez, J. Status and perspectives of  $\text{CO}_2$  conversion into fuels and chemicals by catalytic, photocatalytic and electrocatalytic processes. *Energy Environ. Sci.* **2013**, *6*, 3112–3135.
- (2) Corma, A.; Iborra, S.; Velty, A. Chemical routes for the transformation of biomass into chemicals. *Chem. Rev.* **2007**, *107*, 2411–2502.
- (3) Mika, L. T.; Cséfalvay, E.; Németh, Á. Catalytic conversion of carbohydrates to initial platform chemicals: chemistry and sustainability. *Chem. Rev.* **2018**, *118*, 505–613.
- (4) Torres Galvis, H. M.; Bitter, J. H.; Khare, C. B.; Ruitenbeek, M.; Dugulan, A. I.; de Jong, K. P. Supported iron nanoparticles as catalysts for sustainable production of lower olefins. *Science* **2012**, *335*, 835–838.
- (5) Furukawa, S.; Komatsu, T. Intermetallic compounds: promising inorganic materials for well-structured and electronically modified reaction environments for efficient catalysis. *ACS Catal.* **2017**, *7*, 735–765.
- (6) Carenco, S.; Portehault, D.; Boissière, C.; Mézailles, N.; Sanchez, C. Nanoscaled metal borides and phosphides: recent developments and perspectives. *Chem. Rev.* **2013**, *113*, 7981–8065.
- (7) Roldan Cuenya, B. Metal nanoparticle catalysts beginning to shape-up. *Acc. Chem. Res.* **2013**, *46*, 1682–1691.
- (8) Duan, M.; Yu, J.; Meng, J.; Zhu, B.; Wang, Y.; Gao, Y. Reconstruction of supported metal nanoparticles in reaction conditions. *Angew. Chem., Int. Ed.* **2018**, *57*, 6464–6469.
- (9) Shi, Y.; Zhang, B. Recent advances in transition metal phosphide nanomaterials: synthesis and applications in hydrogen evolution reaction. *Chem. Soc. Rev.* **2016**, *45*, 1529–1541.
- (10) Wang, Y.; Kong, B.; Zhao, D.; Wang, H.; Selomulya, C. Strategies for developing transition metal phosphides as heterogeneous electrocatalysts for water splitting. *Nano Today* **2017**, *15*, 26–55.
- (11) Popczun, E.; McKone, J.; Read, C.; Biacchi, A.; Wiltrout, A.; Lewis, N.; Schaak, R. Nanostructured nickel phosphide as an



electrocatalyst for the hydrogen evolution reaction. *J. Am. Chem. Soc.* **2013**, *135*, 9267–9270.

(12) Cao, S.; Chen, Y.; Wang, C.; He, P.; Fu, W. Highly efficient photocatalytic hydrogen evolution by nickel phosphide nanoparticles from aqueous solution. *Chem. Commun.* **2014**, *50*, 10427–10429.

(13) Liu, P.; Rodriguez, J. Catalysts for hydrogen evolution from the [NiFe] hydrogenase to the Ni<sub>2</sub>P(001) surface: the importance of ensemble effect. *J. Am. Chem. Soc.* **2005**, *127*, 14871–14878.

(14) Liu, T.; Liu, D.; Qu, F.; Wang, D.; Zhang, L.; Ge, R.; Hao, S.; Ma, Y.; Du, G.; Asiri, A.; Chen, L.; Sun, X. Enhanced electrocatalysis for energy-efficient hydrogen production over CoP catalyst with nonelectroactive Zn as a promoter. *Adv. Energy Mater.* **2017**, *7*, 1700020.

(15) De, S.; Zhang, J.; Luque, R.; Yan, N. Ni-based bimetallic heterogeneous catalysts for energy and environmental applications. *Energy Environ. Sci.* **2016**, *9*, 3314–3347.

(16) Yang, S.; Peng, L.; Oveisi, E.; Bulut, S.; Sun, D.; Asgari, M.; Trukhina, O.; Queen, W. MOF-derived cobalt phosphide/carbon nanocubes for selective hydrogenation of nitroarenes to anilines. *Chem. - Eur. J.* **2018**, *24*, 4234–4238.

(17) Liu, K.; Wang, Y.; Chen, P.; Zhong, W.; Liu, Q.; Li, M.; Wang, Y.; Wang, W.; Lu, Z.; Wang, D. Noncrystalline nickel phosphide decorated poly(vinyl alcohol-co-ethylene) nanofibrous membrane for catalytic hydrogenation of p-nitrophenol. *Appl. Catal., B* **2016**, *196*, 223–231.

(18) Gao, R.; Pan, L.; Wang, H.; Zhang, X.; Wang, L.; Zou, J. Ultradispersed nickel phosphide on phosphorus-doped carbon with tailored d-band center for efficient and chemoselective hydrogenation of nitroarenes. *ACS Catal.* **2018**, *8*, 8420–8429.

(19) Carenco, S.; Leyva-Perez, A.; Concepcion, P.; Boissiere, C.; Mezailles, N.; Sanchez, C.; Corma, A. Nickel phosphide nanocatalysts for the chemoselective hydrogenation of alkynes. *Nano Today* **2012**, *7*, 21–28.

(20) Feng, H.; Li, X.; Qian, H.; Zhang, Y.; Zhang, D.; Zhao, D.; Hong, S.; Zhang, N. Efficient and sustainable hydrogenation of levulinic-acid to gamma-valerolactone in aqueous solution over acid-resistant CePO<sub>4</sub>/Co<sub>3</sub>P catalysts. *Green Chem.* **2019**, *21*, 1743–1756.

(21) Fujita, S.; Nakajima, K.; Yamasaki, J.; Mizugaki, T.; Jitsukawa, K.; Mitsudome, T. Unique catalysis of nickel phosphide nanoparticles to promote the selective transformation of biofuranic aldehydes into diketones in water. *ACS Catal.* **2020**, *10*, 4261–4267.

(22) Mitsudome, T.; Sheng, M.; Nakata, A.; Yamasaki, J.; Mizugaki, T.; Jitsukawa, K. A cobalt phosphide catalyst for the hydrogenation of nitriles. *Chem. Sci.* **2020**, *11*, 6682–6689.

(23) Ishikawa, H.; Sheng, M.; Nakata, A.; Nakajima, K.; Yamazoe, S.; Yamasaki, J.; Yamaguchi, S.; Mizugaki, T.; Mitsudome, T. Air-stable and reusable cobalt phosphide nanoalloy catalyst for selective hydrogenation of furfural derivatives. *ACS Catal.* **2021**, *11* (2), 750–757.

(24) Weissmehl, K.; Arpe, H. *Industrial Organic Chemistry*, 3rd ed.; Wiley-VCH, 2008.

(25) Vardanyan, R. S.; Hraby, V. J. *Synthesis of Best-Seller Drugs*; Academic Press, 2016.

(26) Lawrence, S. A. *Amines. Synthesis, Properties and Applications*; Cambridge Univ. Press, 2004.

(27) Gross, T.; Seayad, A. M.; Ahmad, M.; Beller, M. Synthesis of primary amines: First homogeneously catalyzed reductive amination with ammonia. *Org. Lett.* **2002**, *4*, 2055–2058.

(28) Klinckenberg, J. L.; Hartwig, J. F. Catalytic organometallic reactions of ammonia. *Angew. Chem., Int. Ed.* **2011**, *50*, 86–95.

(29) Nakamura, Y.; Kon, K.; Touchy, A. S.; Shimizu, K.; Ueda, W. Selective synthesis of primary amines by reductive amination of ketones with ammonia over supported Pt catalysts. *ChemCatChem* **2015**, *7*, 921–924.

(30) Chatterjee, M.; Ishizaka, T.; Kawanami, H. Reductive amination of furfural to furfurylamine using aqueous ammonia solution and molecular hydrogen: An environmentally friendly approach. *Green Chem.* **2016**, *18*, 487–496.

(31) Komanoya, T.; Kinemura, T.; Kita, Y.; Kamata, K.; Hara, M. Electronic effect of ruthenium nanoparticles on efficient reductive amination of carbonyl compounds. *J. Am. Chem. Soc.* **2017**, *139*, 11493–11499.

(32) Liang, G.; Wang, A.; Li, L.; Xu, G.; Yan, N.; Zhang, T. Production of primary amines by reductive amination of biomass-derived aldehydes/ketones. *Angew. Chem., Int. Ed.* **2017**, *56*, 3050–3054.

(33) Guo, W.; Tong, T.; Liu, X.; Guo, Y.; Wang, Y. Morphology-tuned activity of Ru/Nb<sub>2</sub>O<sub>5</sub> catalysts for ketone reductive amination. *ChemCatChem* **2019**, *11*, 4130–4138.

(34) Jagadeesh, R. V.; Murugesan, K.; Alshammari, A.; Neumann, H.; Pohl, M.; Radnik, J.; Beller, M. MOF-derived cobalt nanoparticles catalyze a general synthesis of amines. *Science* **2017**, *358*, 326–332.

(35) Hahn, G.; Kunas, P.; de Jonge, N.; Kempe, R. General synthesis of primary amines via reductive amination employing a reusable nickel catalyst. *Nat. Catal.* **2019**, *2*, 71–77.

(36) Zhang, Y.; Yang, H.; Chi, Q.; Zhang, Z. Nitrogen-doped carbon-supported nickel nanoparticles: a robust catalyst to bridge the hydrogenation of nitriles and the reductive amination of carbonyl compounds for the synthesis of primary amines. *ChemSusChem* **2019**, *12*, 1246–1255.

(37) Murugesan, K.; Beller, M.; Jagadeesh, R. V. Reusable nickel nanoparticles-catalyzed reductive amination for selective synthesis of primary amines. *Angew. Chem., Int. Ed.* **2019**, *58*, S064–S068.

(38) Bäuml, C.; Bauer, C.; Kempe, R. The synthesis of primary amines through reductive amination employing an iron catalyst. *ChemSusChem* **2020**, *13*, 3110–3114.

(39) Murugesan, K.; Senthamarai, T.; Chandrashekar, V.; Natte, K.; Kamer, P.; Beller, M.; Jagadeesh, R. Catalytic reductive aminations using molecular hydrogen for synthesis of different kinds of amines. *Chem. Soc. Rev.* **2020**, *49*, 6273–6328.

(40) Irrgang, T.; Kempe, R. Transition-metal-catalyzed reductive amination employing hydrogen. *Chem. Rev.* **2020**, *120*, 9583–9674.

(41) Raney, M. Method of preparing catalytic material, U.S. Patent US1563587A, 1925.

(42) Tucker, S. H. Catalytic hydrogenation using Raney nickel. *J. Chem. Educ.* **1950**, *27*, 489–493.

(43) Nishimura, S. *Handbook of heterogeneous catalytic hydrogenation for organic synthesis*; Wiley-VCH, 2001.

(44) Jagadeesh, R. V.; Surkus, A.; Junge, H.; Pohl, M.; Radnik, J.; Rabeah, J.; Huan, H.; Schunemann, V.; Bruckner, A.; Beller, M. Nanoscale Fe<sub>2</sub>O<sub>3</sub>-based catalysts for selective hydrogenation of nitroarenes to anilines. *Science* **2013**, *342*, 1073–1076.

(45) He, L.; Weniger, F.; Neumann, H.; Beller, M. Synthesis, characterization, and application of metal nanoparticles supported on nitrogen-doped carbon: catalysis beyond electrochemistry. *Angew. Chem., Int. Ed.* **2016**, *55*, 12582–12594.

(46) Banerjee, D.; Jagadeesh, R.; Junge, K.; Pohl, M.; Radnik, J.; Brückner, A.; Beller, M. Convenient and mild epoxidation of alkenes using heterogeneous cobalt oxide catalysts. *Angew. Chem., Int. Ed.* **2014**, *53*, 4359–4363.

(47) Jagadeesh, R. V.; Junge, H.; Beller, M. Green synthesis of nitriles using non-noble metal oxides-based nanocatalysts. *Nat. Commun.* **2014**, *5*, 4123.

(48) Chen, F.; Surkus, A.; He, L.; Pohl, M.; Radnik, J.; Topf, C.; Junge, K.; Beller, M. Selective catalytic hydrogenation of heteroarenes with N-graphene-modified cobalt nanoparticles (Co<sub>3</sub>O<sub>4</sub>-Co/NGr@α-Al<sub>2</sub>O<sub>3</sub>). *J. Am. Chem. Soc.* **2015**, *137*, 11718–11724.

(49) Zhang, H.; Ha, D.; Hovden, R.; Kourkoutis, L.; Robinson, R. Controlled synthesis of uniform cobalt phosphide hyperbranched nanocrystals using tri-n-octylphosphine oxide as a phosphorus source. *Nano Lett.* **2011**, *11*, 188–197.

(50) Skála, R.; Drábek, M. The crystal structure of Co<sub>2</sub>P from X-ray powder diffraction data and its mineralogical applications. *Bull. Czech Geol. Surv.* **2001**, *76*, 209–216.

(51) Yuan, Z.; Liu, B.; Zhou, P.; Zhang, Z.; Chi, Q. Preparation of nitrogen-doped carbon supported cobalt catalysts and its application in the reductive amination. *J. Catal.* **2019**, *370*, 347–356.